OPEN ACCESS

Applied Physics Express 17, 071003 (2024) LETTER

https://doi.org/10.35848/1882-0786/ad5c26

Thermal conductivity of $BaZrO_3$ and $KTaO_3$ single crystals

Makoto Tachibana[1*], Cédric Bourgès[2], and Takao Mori[1,3]

[1]Research Center for Materials Nanoarchitechtonics, National Institute for Materials Science, 1-1 Namiki, Tsukuba 305-0044, Japan
[2]International Center for Young Scientists, National Institute for Materials Science, 1-1 Namiki, Tsukuba, 305-0044, Japan
[3]Graduate School of Pure and Applied Sciences, University of Tsukuba, 1-1-1 Tennoudai, Tsukuba 305-8577, Japan

*E-mail: TACHIBANA.Makoto@nims.go.jp

Received June 10, 2024; accepted June 26, 2024; published online July 11, 2024

$BaZrO_3$ and $KTaO_3$ are two rare examples of perovskite oxides that retain the ideal cubic structure down to the lowest temperature. In this paper, we report thermal conductivity (κ) between 300 and 773 K on single crystals of these compounds. For $BaZrO_3$, the κ of 7.5 $Wm^{-1}K^{-1}$ at 300 K is ~40% larger than the previously reported polycrystalline values. For $KTaO_3$, our value of 13.1 $Wm^{-1}K^{-1}$ at 300 K clarifies the sources of error in some of the previously reported data. These results underscore the importance of high-quality experimental data in benchmarking the accuracy of advanced first-principles κ calculations. © 2024 The Author(s). Published on behalf of The Japan Society of Applied Physics by IOP Publishing Ltd

Supplementary material for this article is available online

From the viewpoint of both physical properties and device applications, perovskite oxides ABO_3 are an important group of compounds.[1,2] The perfect perovskite structure has a simple cubic structure (space group $Pm\bar{3}m$), with the B ion at the center of the corner-sharing oxygen octahedron, and the A ion occupying the 12-fold coordinated site between the octahedra. In most perovskites, the cubic structure is realized only at high temperatures, and they undergo one or several structural phase transitions on cooling.[1,2] For example, $BaTiO_3$ and $KNbO_3$ show three sets of ferroelectric (FE) transitions, from cubic to tetragonal $P4mm$ (at 402 and 708 K, respectively) to orthorhombic $Amm2$ (278 and 498 K) to rhombohedral $R3m$ (183 and 263 K). Each of these FE transitions is driven by the condensation of a soft zone-center transverse optic (TO) phonon mode, which displaces the Ti^{4+}/Nb^{5+} ion into a specific direction.[3] Another type of structural transformation is the antiferrodistortive (AFD) rotation of oxygen octahedra, which is associated with the softening and condensation of a zone-boundary mode.[3] $SrTiO_3$ exhibits one such example, where the oxygen octahedra rotate about cubic [001] to form a tetragonal $I4/mcm$ structure below 105 K.[3] Many other perovskites undergo this type of transition, often at very high temperatures ($T > 800$ K).[1,2]

Even when the structure remains cubic down to $T \to 0$ K, as in $BaZrO_3$ and $KTaO_3$, some form of lattice instability is usually found in perovskites. For example, recent neutron and X-ray inelastic scattering measurements[4] on $BaZrO_3$ found softening of the zone-boundary R-point optic mode on cooling, confirming the incipient AFD instability predicted in first-principles calculations.[5,6] Similarly, $KTaO_3$ shows strong softening of the zone-center TO mode, but the anticipated FE transition is suppressed by quantum fluctuations.[7,8] It is interesting to point out that $SrTiO_3$ shows both of these AFD and FE instabilities, the former leading to the transition at 105 K as described above, and the latter remaining incipient due to quantum fluctuations.[7,9]

Because the soft modes arise from strong lattice anharmonicity,[3] a detailed understanding of phonon properties in perovskites remains a challenging problem. Phonon thermal conductivity (κ) is a good example. At room temperature and above, κ in nonmetallic crystals is largely limited by Umklapp phonon-phonon scattering.[10] While basic first-principles κ calculations[11,12] [using interatomic force constants at 0 K from density functional theory (DFT) and three-phonon scattering to solve the Boltzmann transport equation] have been successful in many solids, it is not the case for perovskites.[13] To overcome this problem, recent theoretical studies[14–17] have focused on advanced techniques, such as the self-consistent phonon theory[18] for treating finite temperature effects, incorporation of both three-phonon and four-phonon scattering,[19] and calculation of the off-diagonal terms in the heat flux operators[20] to describe the coherence effects. $BaZrO_3$ and $KTaO_3$ are particularly important materials in this respect, as the structures remain cubic at all temperatures and experimental data are available for checking the κ calculations.

In this study, we report κ between 300 and 773 K on the single crystals of $BaZrO_3$ and $KTaO_3$, based on the flash measurements of thermal diffusivity (D) and the use of reliable heat capacity (C_p) data. Previously, κ of $BaZrO_3$ has been reported on polycrystalline samples,[21–23] and many recent efforts have been aimed at understanding these data from first-principles calculations.[15–17] However, the κ on a single crystal shows a large (~40%) increase from the previous values, indicating that polycrystalline data do not represent intrinsic κ in $BaZrO_3$. For $KTaO_3$, there are disagreements among the reported κ on single crystals,[24–28] and our present data clarify the sources of error in some of the previous measurements. We discuss the implications of these results for studying the κ of perovskites.

High-quality, colorless, and transparent single crystals of $BaZrO_3$ (Refs. 6, 29, 30) and $KTaO_3$ (Ref. 31) were obtained from Crystal Base Co. Ltd. Our crystals were square plates, with 6×6 mm^2 faces and a thickness of 1.01 and 1.03 mm, respectively. The direction of the large faces was {110} for $BaZrO_3$ and {100} for $KTaO_3$. The κ between 300 and 773 K was determined through the relation $\kappa = DC_p\rho$, where ρ is density. The D was obtained in a nitrogen atmosphere by the flash method, using Netzsch LFA 467. In this method, heat is supplied by a flash of light to the front face of a plate specimen, and the temperature at the rear face is recorded as a

function of time. For the measurements, the samples were coated on both sides with a thin layer of graphite, and the model of Mehling et al.[32] was used in the analysis to account for ballistic radiative transfer (photon conduction). The D values (see supplementary data) have an accuracy of ±3%. The C_p of $KTaO_3$ up to 390 K was measured on a smaller single crystal,[24] using the relaxation method of a Quantum Design Physical Property Measurement System (PPMS) with an accuracy of ±1%.[33] The C_p values at higher T, and for $BaZrO_3$ at all T, were determined as described below. For both compounds, literature X-ray values[34,35] were used for ρ at each T. The overall accuracy of our κ at 300 K is ±5%.

We first discuss the C_p data, which are shown in Fig. 1. For $BaZrO_3$, Wang et al.[36] recently provided a table of C_p below 300 K, based on earlier data and their own results from relaxation calorimetry. These values are plotted in Fig. 1. At higher T, the most accurate C_p is usually obtained from drop calorimetry.[37] Several sets of such data are available on $BaZrO_3$, and Tsvetkov et al.[38] gave the recommended values shown in Fig. 1. As these C_p values are deemed to be very reliable, we use these data to obtain the κ for the single crystal. In the previous three κ studies on $BaZrO_3$,[21–23] C_p was determined in each case by differential scanning calorimetry (DSC).[39] While two of these studies[21,22] obtained C_p in reasonable agreement with the present values, the third study by Liu et al.[23] reported C_p that is larger by 8% at 300 K, as shown in Fig. 1. As described below, this discrepancy accounts for their excess κ around 300 K.

For $KTaO_3$, much fewer C_p data are available in the literature. The C_p measured in the present study is plotted with open circles in Fig. 1. Interestingly, the values match those of isostructural $SrTiO_3$ (Ref. 40, from drop calorimetry) between 330 and 390 K, suggesting that we can use the C_p of $SrTiO_3$ up to 773 K as a proxy for $KTaO_3$. With the additional constraint that the C_p must be close to the Dulong-Petit value of 125 $Jmol^{-1}K^{-1}$ at higher T, we expect the accuracy of the present estimate to be better than ∼3%. In any case, these data illuminate the errors in C_p used in previous κ studies: (1) In Ref. 25 Wang et al. used DSC to obtain ∼100 $Jmol^{-1}K^{-1}$ in the entire T region, which is shown with a dotted line in Fig. 1. Although the source of this unusual result is not clear, DSC is known to depend strongly on operator experience[41,42] and can lead to an error of 50% or more.[41] (2) In Ref. 28, Hu et al. used the flash method to measure both D and C_p, the latter shown with open squares in Fig. 1. The C_p obtained by this method often lacks high precision,[41,42] which is evident in this case from the unusual curvature.

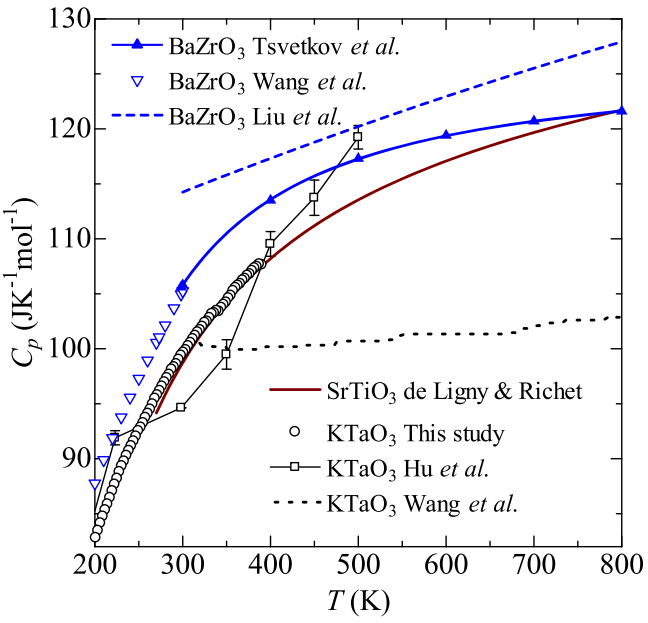

Fig. 1. Heat capacity of $BaZrO_3$ and $KTaO_3$. For $BaZrO_3$, published data from Liu et al.,[23] Wang et al.,[36] and Tsvetkov et al.[38] are shown. The data by Tsvetkov et al.[38] follow $C_p = a + bT + cT^{-2}$, which is shown with a solid line. For $KTaO_3$, the present data and published data from Wang et al.[25] and Hu et al.[28] are shown. See supplementary data for the present data below 200 K. Heat capacity of $SrTiO_3$ from de Ligny and Richet[40] is also shown with a solid line.

We now shift our focus to heat transport. The κ for $BaZrO_3$ is shown in Fig. 2, which includes both the present data on a single crystal and the earlier data on polycrystalline samples.[21–23] As expected for a nonmetallic crystalline solid, each set of data shows a continuous drop in κ with increasing T. The data for the single crystal can be fitted by $\kappa = AT^{-\alpha}$, with $\alpha = 0.74$ giving the best fit. A more significant feature, however, is the much larger κ at 300 K found in the single crystal: the value of 7.5 $Wm^{-1}K^{-1}$ is a 47% and 32% increase from the previous data by Yamanaka et al.[22] and Liu et al.,[23] respectively. We take the comparison with Yamanaka et al.'s data to be more meaningful since Liu et al.'s larger κ below 450 K arises mostly from the excessive C_p (see Fig. 1). Compared to these two polycrystalline data, Vassen et al.'s[21] κ at $T \geqslant 473$ K exhibits much larger values, even overtaking the single crystalline κ above 773 K. The origin of this anomalously large κ is not clear. Nevertheless, its weak T dependence leads to an extrapolated value of ∼6.5 $Wm^{-1}K^{-1}$ at 300 K, which is still significantly lower than the single crystalline value.

The polycrystalline samples of $BaZrO_3$ were dense ceramic pellets prepared using standard techniques,[21–23]

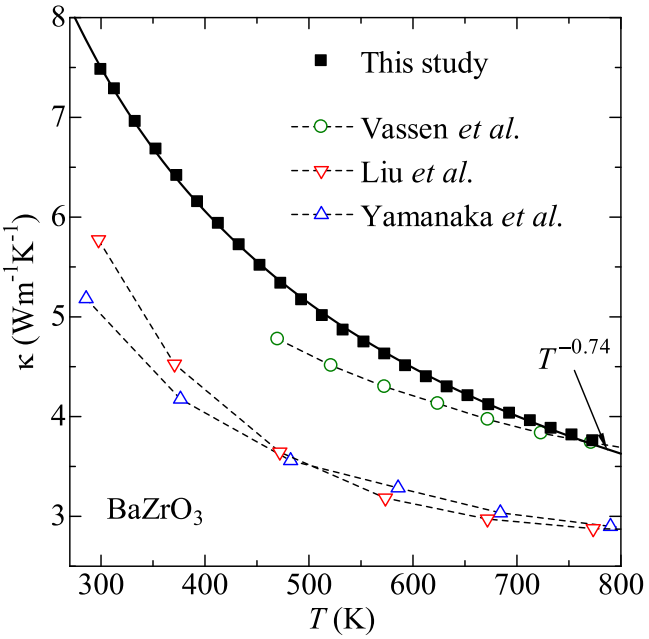

Fig. 2. Thermal conductivity of $BaZrO_3$. The solid line through the present single crystalline data is fit by $\kappa = AT^{-\alpha}$, where $\alpha = 0.74$. Polycrystalline data from Vassen et al.,[21] Yamanaka et al.,[22] and Liu et al.[23] are also shown.

and were composed of μm-sized grains.[23] As the effect of porosity on κ was either negligible[21,23] or corrected,[22] the smaller κ in polycrystals can be ascribed to phonon scattering at grain boundaries. Indeed, a study[43] on $SrTiO_3$ showed a continuous reduction in κ as the grain size was reduced from the bulk single crystal to 20 μm to 55 nm, and our studies[44,45] on $BaTiO_3$ and $LaAlO_3$ also exhibited smaller κ in polycrystals. In this context, it is intriguing to point out that the recent first-principles studies[15–17] on $BaZrO_3$ treated the polycrystalline κ values as intrinsic, without considering the possibility of grain boundary effects. We believe that this state of affairs comes partly from the calculated values of phonon mean free path (MFP): for $BaZrO_3$ and many other perovskites, the dominant MFP is of the order of several nm at 300 K,[15,16] giving an expectation that μm-sized grains do not affect the heat transport. However, it must also be pointed out that the phonon MFP is intrinsically broadband in nature,[10] and there are always some phonons with long MFPs that can be scattered at grain boundaries. At present, much of the theoretical effort[15–17] is aimed at finding the most accurate scheme to calculate κ, which requires reliable experimental data as a benchmark. The present result shows that there is a danger in using polycrystalline data for such a purpose, at least until the grain boundary effects are incorporated into the calculation.

For $KTaO_3$, Fig. 3 compares the present result with other single crystalline data in the literature. Fitting the present data by $\kappa = AT^{-\alpha}$ yields $\alpha = 0.89$, with the fit becoming slightly poorer at the highest T. The first item to note in Fig. 3 is the good agreement between the present data and some of the earlier data, whereas others show much larger differences. The present value of 13.1 $Wm^{-1}K^{-1}$ at 300 K is nearly identical to 13.4 $Wm^{-1}K^{-1}$ by Langenberg et al.,[27] who used the 3ω method to obtain the κ from 20 to 350 K. In the 3ω method,[46] metal lines are fabricated on the surface of the sample, and the third-harmonic voltage is measured while applying an alternating current. Like the flash method used in the present study, the 3ω method does not suffer from large errors due to radiation loss.[46] The excellent agreement between the two data sets attests to the high reliability of these measurement techniques.

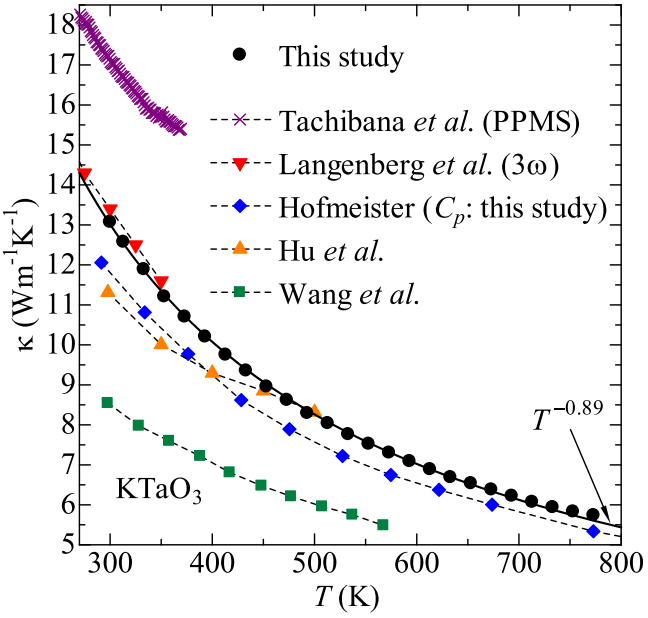

Fig. 3. Thermal conductivity of single crystalline $KTaO_3$. The solid line through the present data is fit by $\kappa = AT^{-\alpha}$, where $\alpha = 0.89$. Published data from Tachibana et al.,[24] Wang et al.,[25] Hofmeister,[26] Langenberg et al.,[27] and Hu et al.[28] are also shown. The κ for Hofmeister is calculated by using the heat capacity from the present study.

Hofmeister[26] and Hu et al.[28] also used the flash method to obtain D. Their D values are lower than our D by 9.7% and 7.7% at 300 K, and 7.5% and 3.2% at 493 K, respectively (see supplementary data). These differences are slightly larger than the combined accuracies, such that variations in crystal quality may also contribute to the difference. However, this level of difference should not be a source of great concern, and we consider these data to be roughly in agreement with each other. In Ref. 28 Hu et al. used the flash method to obtain C_p (see Fig. 1), and the resultant κ is shown in Fig. 3. It is clear that the anomalous curvature in their κ originates from the same feature in C_p. The figure also shows κ based on Hofmeister's D and the present C_p. The good agreement with our κ up to 773 K indicates that spurious contributions from ballistic radiative transfer[26] have been correctly removed in both of these data.

In contrast to these results, much smaller and much larger κ is found in Wang et al.[25] and Tachibana et al.,[24] respectively: (1) Wang et al.[25] used the flash method to obtain D and DSC to obtain C_p. Their D values are lower than our D by 35% at 300 K and 18% at 493 K (see supplementary data). The anomalously low D was already pointed out by Hofmeister and attributed[26] to the relatively thick (2 mm) sample used by Wang et al. As discussed above, Wang et al. 's C_p is also low (see Fig. 1). These values of D and C_p yield the κ shown in Fig. 3, which is evidently much lower than other κ data. (2) Tachibana et al.[24] used the pulse power method[46] of the thermal transport option of the PPMS to obtain the κ between 2 and 370 K. In this method, a heater, two thermometers, and a heat sink are attached along the sample within a radiation shield, and the temperatures are recorded upon application of periodic heat pulses. Like the classic steady-state method, the pulse power method offers a direct κ measurement that can be used down to low T.[46] However, these methods suffer from large radiation losses at high T (>150 K), which are evidenced as a T^3 tail in the raw κ data.[42] Although the PPMS estimates and subtracts this contribution based on the emissivity and surface area of the sample, there is no simple way to verify this correction. Moreover, uncertainties in the sample geometry could also affect the obtained κ. We believe these features of the measurement led to the excessively large κ reported by Tachibana et al.

We have discussed in detail the anomalous results of Tachibana et al.[24] and Wang et al.,[25] because these data happen to be the only ones mentioned in the first-principles κ calculations.[47,48] For example, Fu and Singh[47] performed κ calculations using the local density approximation (LDA) to the DFT and the phonon frequencies fixed at 0 K. With the lattice parameter fully relaxed, they obtained $\kappa = 18$ $Wm^{-1}K^{-1}$ at 300 K and noted on the good agreement with Tachibana et al.'s PPMS data. On the other hand, Fu et al.[48] used the generalized gradient approximation (GGA) to the DFT and calculated the κ under relaxation time approximation (RTA).[11,12] These authors obtained $\kappa = 7.4$ $Wm^{-1}K^{-1}$ at 400 K, and remarked on the excellent

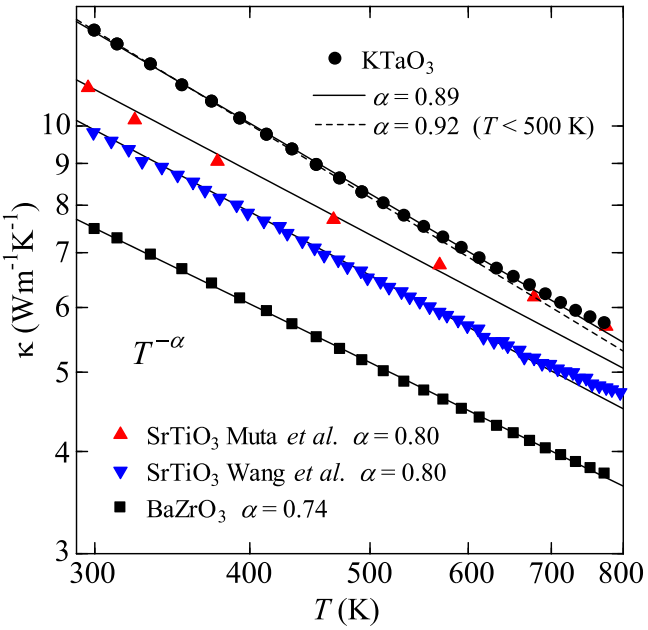

Fig. 4. Thermal conductivity of $BaZrO_3$, $KTaO_3$, and $SrTiO_3$, plotted in logarithmic scales. The data for $SrTiO_3$ are from Wang et al.[43] and Muta et al.[49]

agreement with Wang et al.'s data. In light of Fig. 3, it now appears that these calculations[47,48] did not adequately capture the heat transport in $KTaO_3$. As recent first-principles calculations[8,9] succeeded in reproducing the phonon softening behavior in this compound, it is of great interest to extend such works to calculate the κ and compare the results with those of Fig. 3.

Finally, we provide additional comments on the T dependence and first-principles calculations of κ. In many perovskites, κ is shown to decrease more slowly than the usual T^{-1} dependence.[13] This is one sign that first-principles κ calculations on perovskites require advanced treatments, beyond the basic framework[11,12] of harmonic approximation (HA) and three-phonon (3 ph) scattering. Accordingly, Zhao et al.[15] calculated the κ for many perovskites, with the HA replaced by the self-consistent phonon (SCP) method and four-phonon (4 ph) scattering added to 3 ph scattering. More recently, Zheng et al.[16] focused on $BaZrO_3$ and additionally calculated the off-diagonal (OD) terms in the heat flux operators.[20] In both studies, detailed discussions were made on how the changes in the calculation scheme affect κ and the value of α in the power law $\kappa \propto T^{-\alpha}$. As noted above, the single crystalline data for $BaZrO_3$ obey $\alpha = 0.74$ up to 773 K, and this is more clearly presented with a logarithmic plot in Fig. 4. Interestingly, nearly the same α (0.75) was obtained by the SCP+3,4 ph+OD scheme,[16] which also gave $\kappa = 6.8\ \mathrm{Wm^{-1}K^{-1}}$ at 300 K that is in fair agreement with the experimental value. Thus, the agreement between the calculation and experiment is better than what the authors stated[16] based on polycrystalline data.

For $KTaO_3$, Fig. 4 shows that the present data slightly deviate from the simple $T^{-\alpha}$ behavior; when the upper T limit of the fit is reduced from 773 to 500 K, the obtained α increases from 0.89 to 0.92. If this behavior is an intrinsic property of $KTaO_3$, it could perhaps be associated with the strong T dependence of the soft mode.[8] Alternatively, this behavior may be due to inaccuracies in the D measurement or C_p estimation at high T. To gain a better perspective on this issue, we plot two sets of single crystalline data[43,49] for $SrTiO_3$ in Fig. 4. Here, Wang et al.'s data[43] follow $\alpha = 0.80$ only below 600 K, while Muta et al.'s data[49] do not appear to follow a simple power law at any T. (A solid line with $\alpha = 0.80$ is shown as a reference.) We feel that such uncertainties in experimental α should be more acknowledged in first-principles κ studies, which assume that κ follows a simple $T^{-\alpha}$ behavior up to very high T.[16,17]

Acknowledgments This study was supported by funding from JST-Mirai JPMJMI19A1.

ORCID iDs Makoto Tachibana https://orcid.org/0000-0002-5907-5563 Cédric Bourgès https://orcid.org/0000-0001-9056-0420 Takao Mori https://orcid.org/0000-0003-2682-1846

1) R. H. Mitchell, *Perovskites: Modern and Ancient* (Almaz Press, Ontario, 2002).
2) R. J. Tilley, *Perovskites: Structure-Property Relationships* (Wiley, West Sussex, 2016).
3) M. E. Lines and A. M. Glass, *Principles and Applications of Ferroelectrics and Related Materials* (Clarendon, Oxford, 1977).
4) P. Rosander, E. Fransson, C. Milesi-Brault, C. Toulouse, F. Bourdarot, A. Piovano, A. Bossak, M. Guennou, and G. Wahnström, Phys. Rev. B **108**, 014309 (2023).
5) A. Bilić and J. D. Gale, Phys. Rev. B **79**, 174107 (2009).
6) C. Toulouse, D. Amoroso, C. Xin, P. Veber, M. C. Hatnean, G. Balakrishnan, M. Maglione, P. Ghosez, J. Kreisel, and M. Guennou, Phys. Rev. B **100**, 134102 (2019).
7) K. A. Müller and H. Burkard, Phys. Rev. B **19**, 3593 (1979).
8) L. Ranalli, C. Verdi, L. Monacelli, G. Kresse, M. Calandra, and C. Franchini, Adv. Quantum Technol. **6**, 2200131 (2023).
9) C. Verdi, L. Ranalli, C. Franchini, and G. Kresse, Phys. Rev. Mater. **7**, L030801 (2023).
10) R. Berman, *Thermal Conduction in Solids* (Oxford University Press, Oxford, 1976).
11) A. J.-H. McGaughey, A. Jain, H.-Y. Kim, and B. Fu, J. Appl. Phys. **125**, 011101 (2019).
12) L. Lindsay, Nanoscale Micro. Thermophys. Eng. **20**, 67 (2016).
13) A. van Roekeghem, J. Carrete, C. Oses, S. Curtarolo, and N. Mingo, Phys. Rev. X **6**, 041061 (2016).
14) Q. Wang, Z. Zeng, and Y. Chen, Phys. Rev. B **104**, 235205 (2021).
15) Y. Zhao, S. Zeng, G. Li, C. Lian, Z. Dai, S. Meng, and J. Ni, Phys. Rev. B **104**, 224304 (2021).
16) J. Zheng, D. Shi, Y. Yang, C. Lin, H. Huang, R. Guo, and B. Huang, Phys. Rev. B **105**, 224303 (2022).
17) M. Zeraati, A. R. Oganov, T. Fan, and S. F. Solodovnikov, Phys. Rev. Mater. **8**, 033601 (2024).
18) T. Tadano and S. Tsuneyuki, Phys. Rev. B **92**, 054301 (2015).
19) T. Feng, L. Lindsay, and X. Ruan, Phys. Rev. B **96**, 161201 (2017), (R).
20) P. B. Allen and J. L. Feldman, Phys. Rev. B **48**, 12581 (1993).
21) R. Vassen, X. Cao, F. Tietz, D. Basu, and D. Stöver, J. Am. Ceram. Soc. **83**, 2023 (2000).
22) S. Yamanaka, T. Hamaguchi, T. Oyama, T. Matsuda, S. Kobayashi, and K. Kurosaki, J. Alloys Compd. **359**, 1 (2003).
23) Y. Liu, W. Zhang, B. Wang, L. Sun, F. Li, Z. Xue, G. Zhou, B. Liu, and H. Nian, Ceram. Int. **44**, 16475 (2018).
24) M. Tachibana, T. Kolodiazhnyi, and E. Takayama-Muromachi, Appl. Phys. Lett. **93**, 092902 (2008).
25) X. P. Wang, J. Y. Wang, H. J. Zhang, Y. G. Yu, J. Wu, W. L. Gao, and R. I. Boughton, J. Appl. Phys. **103**, 033513 (2008).
26) A. M. Hofmeister, J. Appl. Phys. **107**, 103532 (2010).
27) E. Langenberg, E. Ferreiro-Vila, V. Leborán, A. O. Fumega, V. Pardo, and F. Rivadulla, APL Mater. **4**, 104815 (2016).
28) L. Hu, D. Sun, H. Zhang, J. Luo, C. Quan, Z. Han, K. Dong, Y. Chen, and M. Cheng, J. Mater. Sci., Mater. Electron. **33**, 13051 (2022).
29) C. Xin et al., CrystEngComm. **21**, 502 (2019).
30) H. A. Helal and S. Kojima, Mater. Sci. Eng. B **271**, 115314 (2021).
31) P. D.-C. King et al., Phys. Rev. Lett. **108**, 117602 (2012).
32) H. Mehling, G. Hautzinger, O. Nilsson, J. Fricke, R. Hofmann, and O. Hahn, Int. J. Thermophys. **19**, 941 (1998).
33) C. A. Kennedy, M. Stancescu, R. A. Marriott, and M. A. White, Cryogenics **47**, 107 (2007).

34) Y. Zhao and D. J. Weidner, Phys. Chem. Minerals **18**, 294 (1991).
35) G. A. Samara and B. Morosin, Phys. Rev. B **8**, 1256 (1973).
36) S. Wang, H. Yan, D. Zhao, Z. Tan, and Q. Shi, J. Chem. Thermodyn. **158**, 106449 (2021).
37) D. A. Ditmars, in *Specific Heat of Solids*, ed. C. Y. Ho, (Hemisphere, New York, 1988).
38) D. S. Tsvetkov, A. L. Sednev-Lugovets, D. A. Malyshkin, V. V. Sereda, A. Y. Zuev, and I. L. Ivanov, J. Phys. Chem. Solids **147**, 109613 (2020).
39) Ref. 23 used Setaram MHTC 96, which can be used for either DSC or drop calorimetry. Ref. 23 did not specify which method was used.
40) D. de Ligny and P. Richet, Phys. Rev. B **53**, 3013 (1996).
41) H. Wang et al., J. Electron. Mater. **42**, 1073 (2013).
42) K. A. Borup et al., Energy Environ, Sci **8**, 423 (2015).
43) Y. Wang, K. Fujinami, R. Zhang, C. Wan, N. Wang, Y. Ba, and K. Koumoto, Appl. Phys. Express **3**, 031101 (2010).
44) M. Tachibana, C. Bourgès, and T. Mori, Appl. Phys. Express **15**, 121003 (2022).
45) M. Tachibana, C. Bourgès, and T. Mori, Appl. Phys. Express **16**, 061003 (2023).
46) D. Zhao, X. Qian, X. Gu, S. A. Jajja, and R. Yang, J. Electron. Packag. **138**, 040802 (2016).
47) Y. Fu and D. J. Singh, Phys. Rev. Mater. **2**, 094408 (2018).
48) Y. Fu et al., Results Phys. **19**, 103591 (2020).
49) H. Muta, K. Kurosaki, and S. Yamanaka, J. Alloys Compd. **392**, 306 (2005).